Reduction of Nitroarenes into Aryl Amines and *N*-Aryl hydroxylamines via Activation of NaBH$_4$ and Ammonia-Borane Complexes by Ag/TiO$_2$ Catalyst

Dimitrios Andreou [1], Domna Iordanidou [1], Ioannis Tamiolakis [2], Gerasimos S. Armatas [2] and Ioannis N. Lykakis [1],*

[1] Department of Chemistry, Aristotle University of Thessaloniki, University Campus, Thessaloniki 54124, Greece; dandreou@chem.auth.gr (D.A.); diordani@chem.auth.gr (D.I.)
[2] Department of Materials Science and Technology, University of Crete, Vassilika Vouton, Heraklion 71003, Greece; gtam@materials.uoc.gr (I.T.); garmatas@materials.uoc.gr (G.S.A.)
* Correspondence: lykakis@chem.auth.gr; Tel./Fax: +30-2310-997-871

Abstract: In this study, we report the fabrication of mesoporous assemblies of silver and TiO$_2$ nanoparticles (Ag/MTA) and demonstrate their catalytic efficiency for the selective reduction of nitroarenes. The Ag/TiO$_2$ assemblies, which show large surface areas (119–128 m$^2 \cdot$g^{-1}) and narrow-sized mesopores (*ca.* 7.1–7.4 nm), perform as highly active catalysts for the reduction of nitroarenes, giving the corresponding aryl amines and *N*-aryl hydroxylamines with NaBH$_4$ and ammonia-borane (NH$_3$BH$_3$), respectively, in moderate to high yields, even in large scale reactions (up to 5 mmol). Kinetic studies indicate that nitroarenes substituted with electron-withdrawing groups reduced faster than those with electron-donating groups. The measured positive ρ values from the formal Hammett-type kinetic analysis of *X*-substituted nitroarenes are consistent with the proposed mechanism that include the formation of possible [Ag]-H hybrid species, which are responsible for the reduction process. Because of the high observed chemo selectivities and the clean reaction processes, the present catalytic systems, *i.e.*, Ag/MTA-NaBH$_4$ and Ag/MTA-NH$_3$BH$_3$, show promise for the efficient synthesis of aryl amines and *N*-aryl hydroxylamines at industrial levels.

Keywords: silver nanoparticles; nitroarenes; aryl amines; *N*-aryl hydroxylamines; titania; heterogeneous catalysis; selective reduction

1. Introduction

Noble metal nanoparticles are well known for their novel applications in the field of catalysis, biotechnology, bio-engineering and environmental remediation [1–5]. In recent years, the synthesis of noble metal nanoparticles as well as their applications, especially in catalysis, is of great interest for further study. Among them, silver nanoparticles (AgNPs) have attracted considerable attention because of their low cost, strong plasmonic properties and superior catalytic activity [6–8]. Several recent efforts to improve the physical properties of AgNPs have focused on synthesis of size- and shape-controlled nanoparticles, which were intended to enhance their catalytic and biological performance [6–11]. However, the practical use of individual AgNPs is often hampered by their severe aggregation during the catalytic reactions. In general, there are two main synthetic routes to overcome these limitations and to obtain small AgNPs with large exposed surface area. One is the surface modification of nanoparticles with organic molecules or surfactants in order to stabilize them against agglomeration and the other is the deposition of nanoparticles on a high-surface-area solid support such as metaloxides (SiO$_2$, TiO$_2$, ZrO$_2$, *etc.*), modified carbons, graphene, or other porous materials. The latter seems to be the most preferred method to sustain the stability and catalytic activity of nanoparticles [6–8]. Ag loaded TiO$_2$

(Ag/TiO$_2$) nanocomposites have recently emerged as promising catalysts for use in organic synthesis, because of the combination between TiO$_2$ electronic and optical properties, and Ag catalytic activities in chemical and biological areas. To this end, a variety of approaches have been used to prepare TiO$_2$ supported Ag catalysts, for instance, by photo deposition, chemical deposition and conventional impregnation method [6–12]. In these studies, however, most of the Ag/TiO$_2$ materials are composed of random aggregates of TiO$_2$ and Ag nanoparticles [6–8]. Moreover, the TiO$_2$ nanoparticles tend to agglomerate into bulk structures leading to a significant decrease in surface area and, therefore, in catalytic activity during repeated reactions.

Thus far, AgNPs have been successfully used as catalysts for several organic transformations, including C–C and C–N cross coupling reactions, cycloaddition and oxidative cyclization reactions, three-component reactions, oxidation of hydrosilanes to silanols, and reduction of imines to the corresponding amines [6–11]. In addition, there are several reports for the synthesis of AgNPs supported on different surfaces, which demonstrated their catalytic activity for the reduction of aromatic nitro compounds to the corresponding amines in the presence of sodium borohydride (NaBH$_4$) as reducing agent [13–22]. To our knowledge, only few examples of AgNPs-based catalyst exhibiting high catalytic activity in nitroarenes reduction have been reported, although excess of NaBH$_4$ or hast conditions (high temperature) are required [8,13–16]. In addition, most of these systems include reduction of nitrophenols by supported AgNPs in aqueous solution [8,17–22].

We recently reported the synthesis of mesoporous TiO$_2$ nanoparticle assemblies (MTA) using a one-pot chemical route. The MTA was prepared through sol-gel polymerization reaction between TiCl$_4$ and Ti(OPr)$_4$ in the presence of polyoxoethylene cetyl ether (Brij-58) block copolymer template [23,24]. Herein, we report the synthesis of new mesoporous hetero structures consisting of titania and silver nanoparticles (Ag/MTA) and demonstrate the catalytic activity of these materials towards the selective reduction of nitroarenes. The obtained Ag/TiO$_2$ assemblies show large internal surface area with narrow pore-size distribution and exhibit extraordinary activity for nitroarenes reduction. We present a systematic study of the reduction of several substituted nitroarenesto the corresponding anilines and *N*-aryl hydroxylamines, using NaBH$_4$ and ammonia-borane (NH$_3$BH$_3$) complexes as the reducing agents. Furthermore, a detailed mechanistic route for the AgNP-catalyzed reduction of nitroarenes in the presence of NaBH$_4$ or NH$_3$BH$_3$ is interpreted on the basis of kinetic analysis, as well as on the products identification by liquid chromatography-mass spectrometry (LC-MS) and nuclear magnetic resonance (NMR) spectroscopy.

2. Results and Discussion

2.1. Structural Properties of Ag/TiO$_2$ Catalysts

In this work, we employed commercial available AgNO$_3$ and AgOTf compounds, Degussa P (25) nanoparticles and mesoporous Ag-loaded TiO$_2$ nanoparticle assemblies (Ag/MTA) as catalysts for the selective reduction of various nitro compounds. All commercial catalysts were used as received. Mesoporous Ag/MTA composites with AgNPs loading amounts of 2, 3, 4 and 7 wt % were prepared by photochemical deposition of AgNPs on the surface of nanoparticle-based mesoporous titania (MTA) [24] (see Supplementary Materials for details). Energy dispersive X-ray spectroscopy (EDS) analysis of the obtained products evidenced that the Ag loadings in the Ag/MTA composites are very close to those expected from the stoichiometry of the reactions (see Table S1, Supplementary Materials).

The mesostructure and crystallinity of the Ag/MTA materials were characterized by X-ray diffraction (XRD), transmission electron microscopy (TEM) and nitrogen physisorption measurements. The powder XRD patterns (Figure S1, Supplementary Materials) indicated the well-defined crystal structure of Ag/MTA. They show a series of intense diffraction peaks in the 2θ = 20°–80° range, which can be assigned to the anatase structure of TiO$_2$ (JCPDS #21-1272). In addition, the XRD patterns of Ag-loaded samples, especially those containing a high Ag loading (>3%), display weak diffractions at ~44.3° (002), ~64.5° (022) and ~77.4° (113), indicating the formation of metallic silver (JCPDS #04-0783).

Figure 1a depicts a representative TEM image of the 4% Ag/MTA sample, which is the most active catalyst studied in this work. It reveals that this material consists of a porous network, which is composed of connected TiO_2 and Ag nanoparticles. On the basis of this technique, the average size of TiO_2 particles was estimated to be *ca.* 7–8 nm, while the diameter of Ag particles was found to be ~3–4 nm. Note that the average diameters of the TiO_2 and Ag nanoparticles were estimated by counting more than 100 particles in several TEM images (Figure S2, Supplementary Materials). To investigate further the crystal structure of mesoporous network, high-resolution TEM (HRTEM) imaging and selected-area electron diffraction (SAED) were performed. The HRTEM images indicate the single-crystal structure of the constituting nanoparticles, showing well-resolved and continuous lattice fringes across the particles. The lattice fringes in Figure 1b,c can be readily assigned to the anatase TiO_2 and face-centered cubic (fcc) Ag structure, respectively, in agreement with the XRD results. From the SAED pattern, it appeared that the crystalline structure of 4% Ag/MTA is a mixture of anatase TiO_2 and cubic Ag. In agreement with XRD and HRTEM results, all the Debye–Scherrer diffraction rings can be reasonably assigned to the anatase phase of TiO_2 (marker by red curves), while the additional diffraction spots could be indexed as (200) and (311) reflections of the cubic Ag (marker by blue dotted cycles) (Figure 1d).
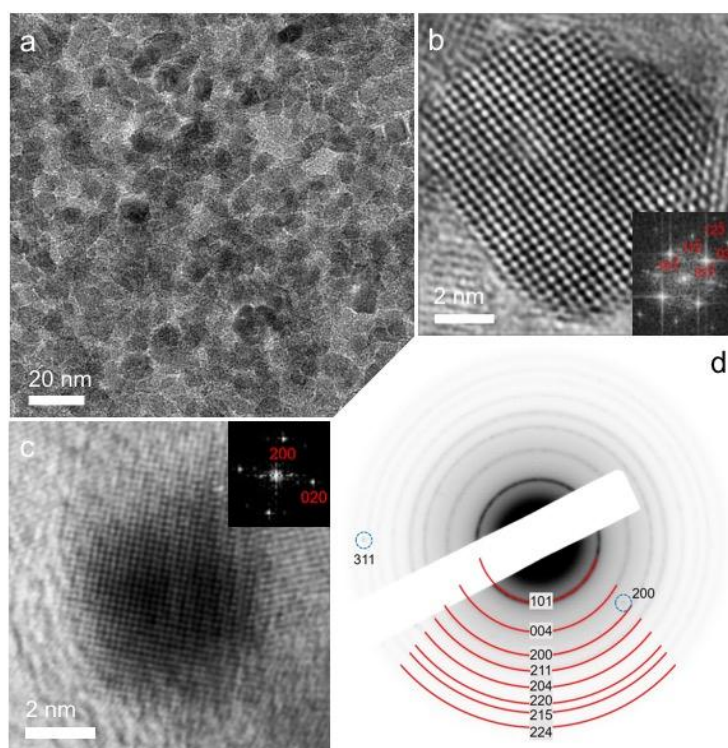

Figure 1. (**a**) Typical transmission electron microscopy (TEM) image; high resolution TEM (HRTEM) of a constituent (**b**) TiO_2 and (**c**) Ag nanoparticle; and (**d**) selected-area electron diffraction (SAED) pattern of mesoporous 4% Ag/mesoporous TiO_2 nanoparticle assemblies (MTA) catalyst. Insets of panels b and c: the corresponding fast Fourier transform (FFT) patterns indexed as the (111) and (100) zone axis diffraction of anatase TiO_2 and face-centered cubic Ag, respectively.

The mesoporosity of the Ag/MTA materials was probed with N_2 physisorption measurements at 77 K. The analysis showed that the Ag/MTA exhibit type-IV adsorption-desorption isotherms with H_2-type hysteresis loop (Figure S3, Supplementary Materials), which correspond to mesoporous materials with narrow-sized pores. The Brunauer-Emmett-Teller (BET) surface area and total pore volume of the Ag/MTA were measured to be 119–128 $m^2 \cdot g^{-1}$ and 0.21–0.23 $cm^3 \cdot g^{-1}$, respectively, which are slightly lower than those of the parent TiO_2 (MTA) sample (surface are ~149 $m^2 \cdot g^{-1}$ and

pore volume ~0.27 $cm^3 \cdot g^{-1}$), probably due to the deposition of AgNPs on the TiO_2 surface. The pore diameter in Ag/MTA samples was obtained by fitting the adsorption isotherms using the non-local density functional theory (NLDFT) model (assuming slit-like pores), and was found to be ~7.1–7.4 nm with narrow pore-size distribution. Furthermore, a weak peak at around 5.4–5.6 nm was observed, especially for the high-Ag-loaded samples (>3 wt %), which could be attributed to the pores filling with AgNPs. Table S1 in the Supplementary Materials summarizes all the textural properties of mesoporous MTA and Ag/MTA materials.

2.2. Evaluation of the Catalytic Activity

Initially, we proceeded to optimize the catalytic conditions by studying the reduction of 4-nitrotoluene (1). In Table 1, we show the yields of 4-toluidine (**1a**) obtained using different Ag-containing catalysts, reducing agents and solvents. Specifically, the catalyst (10 mg) was placed in a 5 mL glass reactor, followed by the addition of solvent (1 mL), nitroarene (0.1 mmol) and hydride compound, and the reaction was vigorous stirred for appropriate time. To our delight, we observed that the 4% Ag/MTA catalyst with 6 mol-excess of $NaBH_4$ in ethanol affords quantitative conversion of **1** into 4-toluidine (**1a**) within 4 h (Table 1, entry 4).Remarkably, no by-products such as azoxy-, azo- or 1,2-diarylhydrazine were detected during the reaction progress by means of ^{1}H-NMR. In comparison, lower reduction yields of **1a** were obtained with Ag/MTA catalysts containing 7 wt % or less than 3 wt % Ag, as shown in Table 1, entries 2, 3 and 5 (see also Supplementary Materials, Figure S4). Meanwhile, TiO_2 alone, such as the MTA mesoporous and Degussa P25 nanoparticles (Table 1, entry 1) are largely inactive for the **1** reduction. Although, $AgNO_3$ and AgOTf catalyzed the conversion of **1** in high yields and short reaction time (Table 1, entries 6 and 7), an equimolar amount of the sesaltsis necessary for the reaction completion. In contrast, silver wire does not catalyze any reduction process (Table 1, entry 8). The reaction was incomplete with lower amounts of $NaBH_4$ (less than 2 mol-excess), while using 4 mol-excess of $NaBH_4$ a prolonged reaction time of 24 h was required to obtain **1a** in >91% yield (results not shown). In addition, no reduction of **1** was observed under mild conditions, for example, using 1 bar of H_2 at room temperature (Table 1, entry 9) or in the presence of transfer hydrogenation reagent such as the 1,1,3,3-tetramethyl disiloxane (TMDS) (Table 1, entry 10). In addition, with dimethylphenylsilane (DMPS), the conversion yield to the corresponding amine (**1a**) was only 11% (Table 1, entry 11). It is also noted that hydrazine hydrate ($NH_2NH_2 \cdot H_2O$) can be activated under our catalytic conditions proceeding to quantitative reduction of **1**, but higher temperature and prolonged reaction time are required (Table 1, entry 12). In contrast, when ammonia-borane (NH_3BH_3) is used as reducing agent (2.5 mol-excess based on **1**) the corresponding *N*-aryl hydroxylamine (**1b**) was detected by ^{1}H-NMR as the major product of **1** reduction, accompanying with small amount of amine **1a** (Table 1, entry 13). Control experiments showed no appreciable reduction of **1** in the absence of catalyst, indicating that the reduction process is catalytic in nature (result not shown). Finally, the reduction of **1** proceeded also efficiently in MeOH (Table 1, entry 14), while in other non-protic polar or apolar solvents no significant amount of **1a** was observed (Table 1, entries 15–19). Thus, 4% Ag/MTA catalyst in the presence of $NaBH_4$ inethanol affords fast, quantitative, and clean reduction of **1** without the requirement of any chromatographic purification of the product **1a** (Table 1, entry 5).After completion of **1**, as evidenced by thin layer chromatography (TLC), the slurry was filtered through a short pad of silica to withhold the catalyst with the aid of ethanol (~5 mL). Then, the filtrate was evaporated under reduced pressure to give pure 4-toluidine **1a** (98% isolated yield) as a brown solid. It is worth noting that our catalytic conditions are significantly milder(room temperature and 6-mol excess of $NaBH_4$) than those used in other studies, in which similar hydrogenation reactions were examined; however, either large excess of $NaBH_4$ (~25–800 mol excess), or hast conditions (>100 °C) are required [13–22]. Based on this, our catalytic system is highly feasible for practical use.
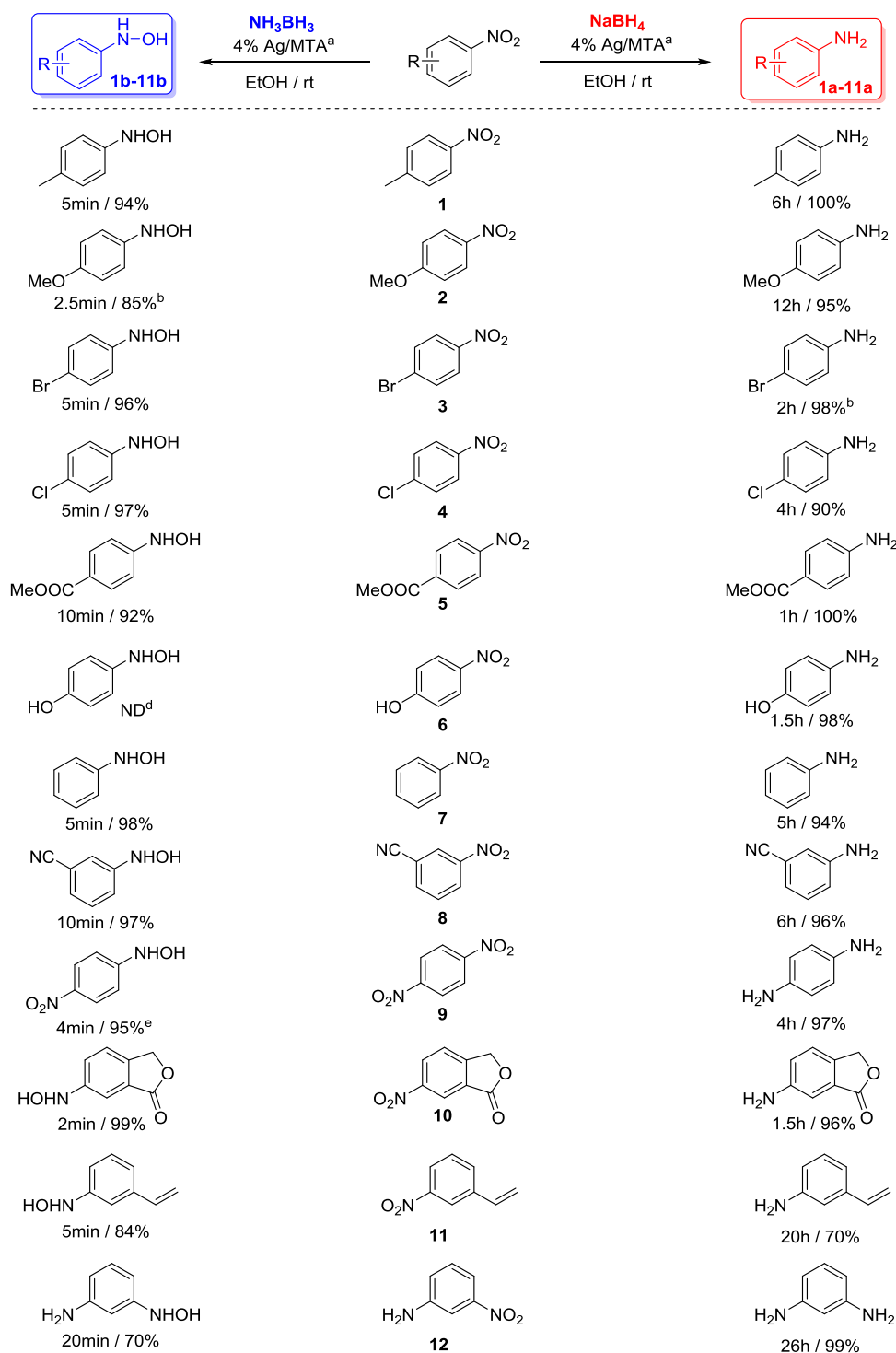
Table 1. Evaluation of various Ag-containing catalysts, reducing agents and solvents in the catalytic reduction of 4-nitrotoluene (**1**) into 4-toluidine (**1a**).

Entry	Catalyst [1]	Solvent	Reducing agent [2]	Time/Yield [3]
1	MTA or P25	EtOH	$NaBH_4$	24h/0%
2	2% Ag/MTA	EtOH	$NaBH_4$	4h/10% [4]
3	3% Ag/MTA	EtOH	$NaBH_4$	4h/51% [4]
4	**4% Ag/MTA**	**EtOH**	**$NaBH_4$**	**4h/>99%**
5	7% Ag/MTA	EtOH	$NaBH_4$	4h/30% [4]
6	AgOTf	EtOH	$NaBH_4$	0.5h/>99% [5]
7	$AgNO_3$	EtOH	$NaBH_4$	0.5h/>99% [5]
8	Ag (wire)	EtOH	$NaBH_4$	24h/0%
9	4% Ag/MTA	EtOH	H_2 (1 atm)	24h/0%
10	4% Ag/MTA	EtOH	TMDS	24h/0%
11	4% Ag/MTA	EtOH	DMPS	4h/11%
12	4% Ag/MTA	EtOH	$NH_2NH_2 \cdot H_2O$	24%/99% [6]
13	**4% Ag/MTA**	**EtOH**	**NH_3BH_3**	**0.2h/6% (94%) [7]**
14	4% Ag/MTA	MeOH	$NaBH_4$	4h/99%
15	4% Ag/MTA	Toluene	$NaBH_4$	4h/0%
16	4% Ag/MTA	THF	$NaBH_4$	4h/0%
17	4% Ag/MTA	CH_3CN	$NaBH_4$	4h/0%
18	4% Ag/MTA	DCM	$NaBH_4$	4h/0%
19	4% Ag/MTA	Acetone	$NaBH_4$	4h/0%

[1] Ten milligrams of each catalyst was used. [2] six mol-excess of $NaBH_4$ were used, while 1,1,3,3-tetramethyl disiloxane (TMDS), dimethylphenylsilane (DMPS) and hydrazine were added in 2.5, 5 and 12 fold-excess of mmols, respectively, based on **1**. [3] Relative yield of **1a** determined by ^{1}H-NMR. [4] The conversions of **1** were in the range of 75%–100%, while the azoxy-, azo- and hydrazo-arenes were formed as major products. [5] Using lower amount of the $AgNO_3$ and AgOTf (20% mol and 50% mol, based on **1**) the conversions of **1** were in the range of 10%–79% after 2h; however, the corresponding hydrazo- and azo-arenes were formed as the major products accompynaning with small amount of the amine **1**. [6] Twelve mol-excess of hydrazine were used for reaction completion at 90 °C. [7] The corresponding *N*-aryl hydroxylamine **1b** was formed as the major product accompanying with small amount of the amine **1a**, within 10 min.

2.3. Chemoselective Reduction of Nitroarenes into Aryl Amines and N-Aryl Hydroxylamines

To study the limitation of this chemoselective reduction process, a series of nitroarenes (**1–12**) were examined under the above described conditions. As shown in Scheme 1, 4% Ag/MTA catalyst in the presence of $NaBH_4$ (6 mol-excess based on nitroarene amount) produce the corresponding substituted anilines **1a–12a** in excellent yields (>90%) and selectivity (>98%). Moreover, bromo and chloro-substituted nitroarenes (**3** and **4**) were also reduced without undergoing any dehalogenation, while *p*-dinitrobenzene (**9**) was completely converted too diamine (**9a**) within 4 h. Similarly, carboxylate, and cyano functionalities in **5** and **8** nitroarenes remained intact under the examined conditions, indicating highly chemoselective reduction. Consistent with the above results, the reduction of 6-nitro-isobenzofuran-1(3*H*)-one (**10**) gave also the corresponding amine without further transformation of the lacton ring. Notably, 3-nitrostyrene **11** was reduced to the corresponding saturated amine **11a** in 70% relative yield, accompanying with a 3-ethyl-nitrobenzene yield of 30% (see Supplementary Materials). This result suggests that the present catalytic system is also active for the preferred hydrogenation of the C=C double bond relative to the nitro group of **11**.

Scheme 1. Chemoselective reduction of nitroarenes (**1–12**) into aryl amines (**1a–12a**) and *N*-aryl hydroxylamines (**1b–12b**) catalyzed by 4% Ag/MTA with NaBH$_4$ and NH$_3$BH$_3$ complexes, respectively.

[a]Ten milligrams of each catalyst was used. In all cases quantitatevaly conversion of the corresponding nitroarene was observed and the percentages below each product correspond to its relative yield determined by ^{1}H-NMR. [b]Totally, 1.5 mol-excess of NH$_3$BH$_3$ was used based on **2** amount. [c]Twenty milligrams of the catalyst were used. [d]Not detected, even at initial reaction time (see also Supplementary Materials). [e]Totally, 2mol-excess of NH$_3$BH$_3$ wasused, based onnitroarene **9** amount.

Nevertheless, when the NH$_3$BH$_3$ (1.5–2.5 mol-excess based on nitroarene amount) is used as the reducing agent, the corresponding *N*-aryl hydroxylamines (**1b–12b**) are formed under the

above described conditions (Scheme 1); indeed, in high relative yields (>84%) and within short reaction times (2–10 min). ^{1}H-NMR analysis of the crude mixtures showed only a small amount of the corresponding substituted anilines (**1a**–**10a**) (2%–10%)as byproducts (see Supplementary Materials). As shown in Scheme 1, the reduction of *p*-nitrophenol (**6**) produces the corresponding amine **6a** as the only product. In this case, *N*-aryl hydroxylamine **6b** was not detected by NMR at initial reaction time (see Supplementary Materials, Figure S5). Reduction of **11** leads to the *N*-aryl hydroxylamine **11b** accompynaning with small amount of the initial nitroarene, however, under the described conditions **12** gave the **12b** in 70% relative yield with a significant amount of the corresponding amine **12a** (30%), (see Supplementary Materials). It should be noted that the reaction products were kept at room temperature and no further chromatographic purification was performed to avoid decomposition or transformation of the *N*-aryl hydroxylamines into the corresponding nitrosoarenes, anilines and azoxy- or azo-arenes. In the literature, several synthetic routes towards *N*-aryl hydroxylamines formation have been reported; however, certain limitations related to the applicability of these reactions (including scale-up synthesis) have been imposed. Since the first procedure using Zn/NH$_4$Cl [25] and the enzymatic nitroreductase system [26], the common synthetic routes associated with the title transformation have focused on the direct hydrogenation (with H$_2$) of nitroarenes using precious metal nanoparticles such as Pd, Pt, Ru, Re and Rh as catalysts [27–33]. In addition, catalytic transfer hydrogenation reactions of nitroarenes to *N*-aryl hydroxylamines were also realized using Pt/hydrazine [34], Zn in CO/H$_2$O [35] and Sb/NaBH$_4$ [36] systems, while only recently Au/TiO$_2$ nanoparticles have been employed for the selective nitroalkanes reduction to *N*-alkyl hydroxylamines [37]. To our knowledge, since now, heterogeneous Ag-catalyzed hydrogenation of nitroarenes to the corresponding *N*-aryl hydroxylamines is an unknown transformation. These results, accompanying with the observation that *N*-aryl hydroxylamines are formed in high relative yields and through afast and pure reaction process, suggest that the present catalytic system Ag/MTA-NH$_3$BH$_3$ can be applicable to various hydrogenation reactions, including fine synthesis of *N*-aryl hydroxylamines.

2.4. Kinetic Studies

The reusability of the 4% Ag/MTA was examined by conducting repeat catalytic experiments. The 4% Ag/MTA catalyst can be easily separated from the reaction mixture by simply filtration and it can be reused for the next catalytic run. As shown in Supplementary Materials, Figure S6, the catalyst can be used at least three times without significant loss of its catalytic activity and selectivity. In order to assess the feasibility of the present catalytic system, the 4% Ag/MTA catalyst was further tested for large-scale production of aryl amines and *N*-aryl hydroxylamines from nitroarenes. For this reason, 5 mmol of nitroarene **1** were reduced in the presence of 4% Ag/MTA (0.8 mol %) with 8 mol-excess of NaBH$_4$ in 15 mL EtOH. After completion of the reaction (within ~20 h based on TLC analysis), the mixture was filtered upon silica gel, washed with ethanol and purified by column chromatography to afford the corresponding 4-toluedine **1a** in 91% isolated yield. As a comparison, under the same reaction conditions but with 3 mol-excess of NH$_3$BH$_3$, the corresponding *N*-aryl hydroxyamine **1b** was obtained at 93% relative yield in 30 min, according to the ^{1}H-NMR analysis of the crude product (results not shown). These results correspond to a turn over number (TON) of about 125 and a turnover frequency (TOF) of 250 h^{-1}.

To propose a plausible mechanistic pathway for the present Ag-catalyzed reduction of nitroarenes, we performed a Hammett-type kinetic study for the reduction of a diverse set of *para-* and meta-*X*-substituted-nitroarenes (**1**, **2**, **3**, **4**, **5**, **7**, **8** and **12**). The kinetic studies were carried out as follow: 0.2 mmol of the nitroarene, 20 mg of 4% Ag/MTA and 0.6 mmol of NaBH$_4$ were added in ethanol (1 mL). A 100 μL aliquot of the mixture was taken at appropriate time and the mixture was filtrated through a short pad of silica (to withhold the catalyst) and washed with ethanol (~1 mL). Then, the filtrate was evaporated under reduced pressure and the consumptions of the corresponding *X*-substituted nitroarene were determined by integrating the appropriate proton signals in ^{1}H-NMR

spectra. Each reaction was repeated at least three times and the average values are depicted in Figure 2 and in the Supplementary Materials, Figures S7 and S8. Considering that the concentration of the possible formed silver-hydride species remains constant at initial times and assuming a pseudo-first order dependence of the reaction rate on the nitroarene concentration, Equation (1) can be applied.

$$\ln(x) = -kt \tag{1}$$

where, k is the rate constant and x is the consumption of the X-substituted nitroarene at reaction time t.
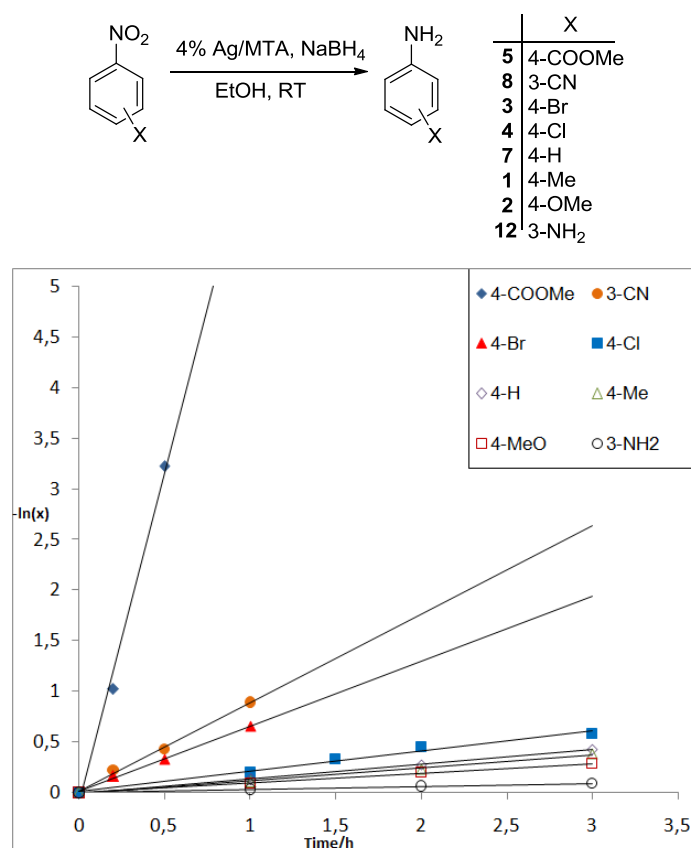

Figure 2. Kinetic analysis of the 4% Ag/MTA-catalyzed reduction of various X-substituted nitroarenes (X = 3-NH$_2$ (**12**), 4-MeO (**2**), 4-Me (**1**), 4-Br (**3**), 4-H (**7**), 4-Cl (**4**), 3-CN (**8**) and 4-COOMe (**5**)) with NaBH$_4$.

According to Equation (1), a plot of the $\ln(x)$ *versus* time gives a linear curve, the slope of which is equal to the rate constant k. The results indicated that the kinetic activity of **1**, **2**, **3**, **4**, **5**, **7**, **8** and **12** nitroarenes is remarkably affected by the nature of the X-substituent group, in which the reduction proceeds faster as the electron-withdrawing ability of the substituent group increases. For example, the reduction of **3** (4-Br), **4** (4-Cl), **5** (4-COOMe) and **8** (3-CN) proceeds in a faster rate than that with the nitrobenzene **7** (X = H) (Figure 2), as indicated by the relative rate constant ratios $k_{COOMe}/k_H = 25$, $k_{CN}/k_H = 6.0$, $k_{Br}/k_H = 4.5$ and $k_{Cl}/k_H = 1.4$, respectively (see also Supplementary Materials, Figures S7 and S8). However, nitroarenes containing electron-donating group, such as **12** (3-NH$_2$), **2** (4-MeO) and **1** (4-Me), were reduced with slower reaction rate (Figure 2); the relative rate constant rations were $k_{NH2}/k_H = 0.2$, $k_{MeO}/k_H = 0.7$ and $k_{Me}/k_H = 0.9$, respectively. In addition to these results, a Hammett-type correlation in the competition of X-substituted nitroarenes (**12**, **2**, **1**, **4**, **3**, **8** and **5**) *versus* nitrobenzene (**7**) gave positive slopes, *i.e.*, $\rho \approx 0.8$, $R^2 = 0.890$ (using σ^+ values) and $\rho \approx 0.9$, $R^2 = 0.826$ (using σ values) (Supplementary Materials, Figure S9). The small ρ values for these correlations indicate that the reaction mechanism involves either radical intermediates or a transition state with a small charge separation [38]. However, the measured positive ρ values, are consistent

with a proposed mechanism that include a negative charge (or hydride transfer) in the transition state, which is stabilized by electron-withdrawing substituents [38,39].

According to the above results, we propose a general mechanistic pathway for the AgNPs catalyzed reduction of nitroarenes. First, a B-H bond cleavage occurs to gives [Ag]-H active species. Such hybrid species are responsible for the rapid reduction of nitroarenes into the corresponding *N*-aryl hydroxylamines. This assumption is consistent with the kinetics studies showing that nitroarenes bearing electron-withdrawing substituents reduced faster than those with electron donating groups. Finally, *N*-aryl hydroxylamines are further reduced into the corresponding aryl amines with $NaBH_4$; however, this step becomes slower in the presence of NH_3BH_3. To shed light on the above hypothesis, the catalytic reductions of electron-donating **2** and electron-withdrawing **5** and **9** *p-X*-substituted nitroarenes were also separately conducted in CD_3OD using 4% Ag/MTA. Each reduction process was monitored directly by ^{1}H-NMR spectroscopy, at initial reaction times. As shown in Figures S10–S12 of the Supplementary Materials, during the reduction process, the only intermediate products were the corresponding *N*-aryl hydroxylamines **2b**, **5b** and **9b**.

3. Experimental Section

3.1. Materials

Brij 58 surfactant ($HO(CH_2CH_2O)_{20}C_{16}H_{33}$, Mn~1124), titanium tetrachloride (99.9%), $AgNO_3$ (>99%), AgOTf, absolute ethanol (99.8%), $NaBH_4$, NH_3BH_3, TMDS and DMPS were purchased from Sigma-Aldrich (Darmstadt, Germany). Titanium(IV) isopropoxide (>98%) was purchased from Merck (Darmstadt, Germany). TiO_2 nanoparticles (P25) were purchased from Degussa AG (Dusseldorf, Germany).The aromatic nitro compounds used as substrates were of high purity and commercially available from Aldrich (Darmstadt, Germany).

3.2. Synthesis of Ag/MTA Catalysts

The mesoporous TiO_2 nanoparticle assemblies (MTA) were prepared according to the method reported previous [24]. Ag-loaded TiO_2 (Ag/MTA) catalysts with different loading of AgNPs were obtained by photocatalytic reduction method. Typically, 0.2 g of MTA were dispersed into 10 mL of a CH_3CN/H_2O/ethanol (10:1:1 *v/v*) solution containing appropriate amounts of $AgNO_3$. The suspension was then illuminated with a 5 mW ultraviolet lamp (λ = 365 nm) for 2 h under continuous stirring. The product was then collected by filtration, washed with ethanol, and dried at 60 $^\circ$C for 12 h. A series of mesoporous Ag/MTA catalysts with different Ag loadings, *i.e.*, *x* = 2, 3, 4 and 7 wt %, was prepared using 6.4, 9.6, 13.2 and 23.8 mg of $AgNO_3$, respectively.

3.3. Physical Characterization

The X-ray diffraction (XRD) patterns were collected using a Panalytical X'Pert Pro MPD X-ray diffractometer (45 kV and 40 mA, Lelyweg, the Netherlands) with a Cu Kα radiation (λ = 1.5406 Å). Elemental microprobe analysis was performed on a JEOL Model JSM-6390LV scanning electron microscopy (SEM, Tokyo, Japan) system equipped with an Oxford INCA PentaFET-x3 energy-dispersive X-ray spectroscopy (EDS) detector (Oxfordshire, UK). Data acquisition was performed several times using an accelerating voltage of 20 kV and 60 s accumulation time. Transmission electron microscopy (TEM) experiments were carried out with a JEOL model JEM-2100 electron microscope (LaB$_6$ filament) operating at 200 kV. The sample was dispersed in ethanol by sonication, and the dispersion was then dropped onto a Cu grid covered with carbon film. Nitrogen adsorption-desorption isotherms were measured at liquid N_2 temperature (77 K) on a NOVA 3200e volumetric analyzer (Quantachrome, Boynton Beach, FL, USA). Before analysis, samples were degassed overnight at 150 $^\circ$C under vacuum (<10^{-5} Torr) to remove moisture. The specific surface areas were calculated using the Brumauer-Emmett-Teller (BET) method [40] on the adsorption data in the 0.06–0.25 relative pressure (P/P_o) range. The total pore volumes were derived from the adsorbed volume at

P/P_o = 0.99 and the pore size distributions were obtained by the nonlocal density functional theory (NLDFT) method [41] based on the adsorption data.

3.4. Catalytic Reactions

Supported silver catalyst Ag/MTA (10 mg) was placed in a 5 mL glass reactor, followed by the addition of ethanol (1 mL), nitro compound (0.1 mmol) and $NaBH_4$ (0.6 mmol) or NH_3BH_3 (0.25 mmol), and the reaction mixture was stirred at room temperature for a selected time. The reaction was monitored by thin layer chromatography (TLC), and after completion, the slurry was filtered under pressure through a short pad of silica to withhold the catalyst with the aid of ethanol or methanol (~5 mL). After solvent evaporation the corresponding products were formed in pure forms. Product analysis was conducted by ^{1}H-NMR and ^{13}C-NMR spectroscopy (Bruker AM 300, Bruker Biospin GMBH, Rheinstetten, Germany and Agilent AM 500, Agilent Technologies, Santa Clara, CA, USA). Identification of the products was realized by comparing the NMR spectra with those of the commercially available pure substances. LC-MS 2010 EV Instrument (Shimadzu, Tokyo, Japan) under Electrospray Ionization (ESI) conditions was used for the determination of the mass spectra.

Reusability testing of the catalyst was conducted in the case of the 4% Ag/MTA sample through the reduction of 4-nitrotoluene (1). A 2 mL mixture of the feeding solution (0.2 mmol of **1**, 1.2 mmol of $NaBH_4$ and 20 mg of catalyst (4 mol % Ag)) was placed into a vial. Each catalytic reaction was stopped after 6 h and the catalyst was collected by filtration, washed with ethanol and dried in an oven at 100 °C for 12 h. Then, the recovered catalyst was used for the next catalytic run without any additional treatment.

4. Conclusions

In conclusion, we have shown that mesoporous titania supported silver nanoparticles (Ag/MTA) can effectively catalyze the chemoselective reduction of nitroarenes into the corresponding aryl amines and *N*-aryl hydroxylamines, employing $NaBH_4$ and NH_3BH_3 as reducing agents, respectively. Product analysis and kinetic studies indicated that aryl amine formation proceeds through a reduction pathway involving the initial formation of silver-hydride species; although additional mechanistic studies are required in this direction. In both catalytic processes, the corresponding *N*-aryl hydroxylamines were observed either as intermediates (with $NaBH_4$) or as the major products (with NH_3BH_3). Based on the observed high chemoselectivities and the fast and clean reaction processes, both catalytic systems, Ag/MTA-$NaBH_4$ and Ag/MTA-NH_3BH_3, can be applicable to various hydrogenation reactions, including fine synthesis of amines and *N*-aryl hydroxylamines, respectively.

Author Contributions: D.A., D.I. and I.T. designed and performed all the experiments and interpretation of results. G.S.A. and I.N.L supervised this work, prepared and reviewed the manuscript.

Conflicts of Interest: The authors declare no conflict of interest.

References

1.　Chaudhuri, R.G.; Paria, S. Core/shell nanoparticles: Classes, properties, synthesis mechanisms, characterization, and applications. *Chem. Rev.* **2012**, *112*, 2373–2433. [CrossRef] [PubMed]

2.　Sreeprasad, T.S.; Pradeep, T. Noble metal nanoparticles. In *Springer Handbook of Nanomaterials*; Vajtai, R., Ed.; Springer-Verlag: Berlin, Germany, 2013; pp. 303–388.

3.　Astruc, D. Transition-metal nanoparticles in catalysis: From historical background to the state-of-the art. In *Nanoparticles and Catalysis*; Astruc, D., Ed.; Wiley-VCH Verlag GmbH and Company KGaA: Weinheim, Germany, 2008; pp. 1–48.

4. Doria, C.; Conde, J.; Veigas, B.; Giestas, L.; Almeida, C.; Assunção, M.; Rosa, J.; Baptista, P.V. Noble metal nanoparticles for biosensing applications. *Sensor* **2012**, *12*, 1657–1687. [CrossRef] [PubMed]

5. De, M.; Ghosh, P.S.; Rotello, V.M. Applications of nanoparticles in biology. *Adv. Mater.* **2008**, *20*, 4225–4241. [CrossRef]

6. El-Nour, K.M.M.A.; Eftaiha, A.; Al-Warthan, A.; Ammar, R.A.A. Synthesis and applications of silver nanoparticles. *Arabian J. Chem.* **2010**, *3*, 135–140. [CrossRef]

7. Tran, Q.H.; Nguyen, V.Q.; Le, A.-T. Silver nanoparticles: Synthesis, properties, toxicology, applications and perspectives. *Adv. Nat. Sci. Nanosci. Nanotechnol.* **2013**, *4*. [CrossRef]

8. Bhosale, M.A.; Bhanage, B.M. Silver nanoparticles: Synthesis, characterization and their application as a sustainable catalyst for organic transformations. *Curr. Org. Chem.* **2015**, *19*, 708–727. [CrossRef]

9. Abbiati, G.; Rossi, E. Silver and gold-catalyzed multicomponent reactions. *Beilstein J. Org. Chem.* **2014**, *10*, 481–513. [CrossRef] [PubMed]

10. Rycnge, M.; Cobley, C.M.; Zeng, J.; Li, W.; Moran, C.H.; Zhang, Q.; Qin, D.; Xia, Y. Controlling the synthesis and assembly of silver nanostructures for plasmonic applications. *Chem. Rev.* **2011**, *111*, 3669–3712.

11. Dong, X.-Y.; Gao, Z.-W.; Yang, K.-F.; Zhang, W.-Q.; Xu, L.-W. Nanosilver as a new generation of silver catalysts in organic transformations for efficient synthesis of fine chemicals. *Catal. Sci. Technol.* **2015**, *5*, 2554–2574. [CrossRef]

12. Kundu, S.; Mandal, M.; Ghosh, S.K.; Pal, T. Photochemical deposition of SERS active silver nanoparticles on silica gel and their application as catalysts for the reduction of aromatic nitro compounds. *J. Colloid Interface Sci.* **2004**, *272*, 134–144. [CrossRef] [PubMed]

13. Davarpanah, J.; Kiasat, A.R. Catalytic application of silver nanoparticles immobilized to rice husk-SiO$_2$-aminopropylsilane composite as recyclable catalyst in the aqueous reduction of nitroarenes. *Catal. Commun.* **2013**, *41*, 6–11. [CrossRef]

14. Solanki, J.N.; Murthy, Z.V.P. Reduction of nitro aromatic compounds over Ag/Al$_2$O$_3$ nanocatalyst prepared in water-in-oil microemulsion: Effects of water-to-surfactant mole ratio and type of reducing agent. *Ind. Eng. Chem. Res.* **2011**, *50*, 7338–7344. [CrossRef]

15. Zhou, Q.; Qian, G.; Li, Y.; Zhao, G.; Chao, Y.; Zheng, J. Two-dimensional assembly of silver nanoparticles for catalytic reduction of 4-nitroaniline. *Thin Solid Films* **2008**, *516*, 953–956. [CrossRef]

16. Pradhan, N.; Pal, A.; Pal, T. Silver nanoparticle catalyzed reduction of aromatic nitro compounds. *Colloids Surf. A* **2002**, *196*, 247–257. [CrossRef]

17. Dong, Z.; Le, X.; Li, X.; Zhang, W.; Dong, C.; Ma, J. Silver nanoparticles immobilized on fibrous nano-silica as highly efficient and recyclable heterogeneous catalyst for reduction of 4-nitrophenol and 2-nitroaniline. *Appl. Catal. B* **2014**, *158*, 129–135. [CrossRef]

18. Chi, Y.; Tu, J.; Wang, M.; Li, X.; Zhao, Z. One-pot synthesis of ordered mesoporous silver nanoparticle/carbon composites for catalytic reduction of 4-nitrophenol. *J. Colloid Interface Sci.* **2014**, *423*, 54–59. [CrossRef] [PubMed]

19. Deshmukh, S.P.; Dhokale, R.K.; Yadav, H.M.; Achary, S.N.; Delekar, S.D. Titania-supported silver nanoparticles: An efficient and reusable catalyst for reduction of 4-nitrophenol. *Appl. Surf. Sci.* **2013**, *273*, 676–683. [CrossRef]

20. Wang, M.; Tian, D.; Tian, P.; Yuan, L. Synthesis of micron-SiO$_2$@nano-Ag particles and their catalyticperformance in 4-nitrophenol reduction. *Appl. Surf. Sci.* **2013**, *283*, 389–395. [CrossRef]

21. Mohamed, M.M.; Al-Sharif, M.S. One pot synthesis of silver nanoparticles supported on TiO$_2$ using hybrid polymers as template and its efficient catalysis for the reduction of 4-nitrophenol. *Mater. Chem. Phys.* **2012**, *136*, 528–537. [CrossRef]

22. Jiang, H.-L.; Akita, T.; Ishida, T.; Haruta, M.; Xu, Q. Synergistic catalysis of Au@Ag core-shell nanoparticles stabilized on metal-organic framework. *J. Am. Chem. Soc.* **2011**, *133*, 1304–1306. [CrossRef] [PubMed]

23. Tamiolakis, I.; Fountoulaki, S.; Vordos, N.; Lykakis, I.N.; Armatas, G.S. Mesoporous Au-TiO$_2$ nanoparticle assemblies as efficient catalysts for the chemoselective reduction of nitro compounds. *J. Mater. Chem. A* **2013**, *1*, 14311–14319. [CrossRef]

24. Tamiolakis, I.; Lykakis, I.N.; Katsoulidis, A.P.; Armatas, G.S. One-pot synthesis of highly crystalline mesoporous TiO$_2$ nanoparticle assemblies with enhanced photocatalytic activity. *Chem. Commun.* **2012**, *48*, 6687–6689. [CrossRef] [PubMed]

25. Kamm, O. β-phenylhydroxylamines. *Org. Synth.* **1925**, *4*, 57–58.

26.　Nguyen-Tran, H.-H.; Zheng, G.-W.; Qian, X.-H.; Xu, J.-H. Highly selective and controllable synthesis of arylhydroxylamines by the reduction of nitroarenes with an electron-withdrawing group using a new nitroreductase *Ba*NTR1. *Chem. Commun.* **2014**, *50*, 2861–2864. [CrossRef] [PubMed]

27.　Boymans, E.H.; Witte, P.T.; Vogt, D. A study on the selective hydrogenation of nitroaromatics to *N*-arylhydroxylamines using a supported Pt nanoparticle catalyst. *Catal. Sci. Technol.* **2015**, *5*, 176–183. [CrossRef]

28.　Rong, Z.; Du, W.; Wang, Y.; Lu, L. Carbon supported Pt colloid as effective catalyst for selective hydrogenation of nitroarenes to arylhydroxylamines. *Chem. Commun.* **2010**, *46*, 1559–1561. [CrossRef] [PubMed]

29.　Takenaka, Y.; Kiyosu, T.; Choi, J.C.; Sakakura, T.; Yasuda, H. Selective synthesis of *N*-aryl hydroxylamines by the hydrogenation of nitroaromatics using supported platinum catalysts. *Green Chem.* **2009**, *11*, 1385–1390. [CrossRef]

30.　Pernoud, L.; Candy, P.; Didillon, B.; Jacquot, R.; Basset, J.M. *Studies in Surface Science and Catalysis*; Avelino Corma, F.V.M.S.M., José Luis, G.F., Eds.; Elsevier: Amsterdam, the Netherlands, 2000; Volume 130, pp. 2057–2062.

31.　Tamura, M.; Kon, K.; Satsuma, A.; Shimizu, K. Volcano-curves for dehydrogenation of 2-propanol and hydrogenation of nitrobenzene by SiO_2-supported metal nanoparticles catalysts as described in terms of a d-band model. *ACS Catal.* **2012**, *2*, 1904–1909. [CrossRef]

32.　Widegren, J.A.; Finke, R.G. A review of soluble transition-metal nanoclusters as arene hydrogenation catalysts. *J. Mol. Catal. A* **2003**, *191*, 187–207. [CrossRef]

33.　Karwa, S.L.; Rajadhyaksha, R.A. Selective catalytic hydrogenation of nitrobenzene to phenylhydroxylamine. *Ind. Eng. Chem. Res.* **1987**, *26*, 1746–1750. [CrossRef]

34.　Shila, A.K.; Das, P. Solid supported platinum(0) nanoparticles catalyzed chemo-selective reduction of nitroarenes to *N*-arylhydroxylamines. *Green Chem.* **2013**, *15*, 3421–3428. [CrossRef]

35.　Liu, S.; Wang, Y.; Jianga, J.; Jina, Z. The selective reduction of nitroarenes to *N*-arylhydroxylamines using Zn in a CO_2/H_2O system. *Green Chem.* **2009**, *11*, 1397–1400. [CrossRef]

36.　Ren, P.; Dong, T.; Wu, S. Synthesis of *N*-arylhydroxylamines by antimony-catalyzed reduction of nitroarenes. *Synth. Commun.* **1997**, *27*, 1547–1552. [CrossRef]

37.　Vasilikogiannaki, E.; Gryparis, C.; Kotzabasaki, V.; Lykakis, I.N.; Stratakis, M. Facile reduction of nitroarenes into anilines and nitroalkanes into hydroxylamines via the rapid activation of ammonia-borane complex by supported gold nanoparticles. *Adv. Synth. Catal.* **2013**, *355*, 907–911. [CrossRef]

38.　Lowry, T.H.; Richardson, K.S. *Mechanism and Theory in Organic Chemistry*, 3rd ed.; Harper & Row: New York, NY, USA, 1987; pp. 60–71.

39.　Fountoulaki, S.; Daikopoulou, V.; Gkizis, P.L.; Tamiolakis, I.; Armatas, G.S.; Lykakis, I.N. Mechanistic studies of the reduction of nitroarenes by $NaBH_4$ or hydrosilanes catalyzed by supported gold nanoparticles. *ACS Catal.* **2014**, *4*, 3504–3511. [CrossRef]

40.　Brunauer, S.; Deming, L.S.; Deming, W.E.; Teller, E. On a theory of the van der Waals adsorption of gases. *J. Am. Chem. Soc.* **1940**, *62*, 1723–1732. [CrossRef]

41.　Ravikovitch, P.I.; Wei, D.; Chueh, W.T.; Haller, G.L.; Neimark, A.V. Evaluation of pore structure parameters of MCM-41 catalyst supports and catalysts by means of nitrogen and argon adsorption. *J. Phys. Chem. B* **1997**, *101*, 3671–3679. [CrossRef]